

Received September 13, 2019, accepted September 24, 2019, date of publication September 30, 2019, date of current version October 16, 2019.

Digital Object Identifier 10.1109/ACCESS.2019.2944691

Epileptic Seizure Forecasting With Generative Adversarial Networks

NHAN DUY TRUONG^{1,2}, (Student Member, IEEE), LEVIN KUHLMANN^{3,4}, MOHAMMAD REZA BONYADI⁵, (Senior Member, IEEE), DAMIEN QUERLIOZ⁶, (Member, IEEE), LUPING ZHOU¹, (Senior Member, IEEE), AND OMID KAVEHEI^{1,2}, (Senior Member, IEEE)

¹Faculty of Engineering, The University of Sydney, Camperdown, NSW 2006, Australia

²The University of Sydney Nano Institute, Camperdown, NSW 2006, Australia

³Faculty of Information Technology, Monash University, VIC 3800, Australia

⁴Department of Medicine, St. Vincent's Hospital Melbourne, The University of Melbourne, Fitzroy, VIC 3065, Australia

⁵Centre for Advanced Imaging, The University of Queensland, St. Lucia, QLD 4072, Australia

⁶Center for Nanoscience and Nanotechnology, CNRS, Université Paris-Sud, Université Paris-Saclay, 91405 Orsay, France

Corresponding author: Omid Kavehei (omid.kavehei@sydney.edu.au)

This work was supported in part by the Sydney Research Accelerator (SOAR) Fellowship and an Early Career Research Grant through The University of Sydney, and in part by the Sydney Informatics Hub through the University of Sydney's Core Research Facilities. The work of N. D. Truong was supported by providing John Makepeace Bennett Gift Scholarship through the Australian Institute for Nanoscale Science and Technology (AINST) and administered by the University of Sydney Nano Institute.

ABSTRACT Many outstanding studies have reported promising results in seizure forecasting, one of the most challenging predictive data analysis problems. This is mainly because electroencephalogram (EEG) bio-signal intensity is very small, in μ V range, and there are significant sensing difficulties given physiological and non-physiological artifacts. Today the process of accurate epileptic seizure identification and data labeling is done by neurologists. The current unpredictability of epileptic seizure activities together with the lack of reliable treatment for patients living with drug resistant forms of epilepsy creates an urgency for research into accurate, sensitive and patient-specific seizure forecasting. Most seizure forecasting algorithms use only labeled data for training purposes. As the seizure data is labeled manually by neurologists, preparing the labeled data is expensive and time consuming, making the best use of the data critical. In this article, we propose an approach that can make use of not only labeled EEG signals but also the unlabeled ones which are more accessible. We use the short-time Fourier transform on 28-s EEG windows as a pre-processing step. A generative adversarial network (GAN) is trained in an unsupervised manner where information of seizure onset is disregarded. The trained Discriminator of the GAN is then used as a feature extractor. Features generated by the feature extractor are classified by two fully-connected layers (can be replaced by any classifier) for the labeled EEG signals. This semi-supervised patient-specific seizure forecasting method achieves an out-of-sample testing area under the operating characteristic curve (AUC) of 77.68%, 75.47% and 65.05% for the CHB-MIT scalp EEG dataset, the Freiburg Hospital intracranial EEG dataset and the EPILEPSIAE dataset, respectively. Unsupervised training without the need for labeling is important because not only it can be performed in real-time during EEG signal recording, but also it does not require feature engineering effort for each patient. To the best of our knowledge, this is the first application of GAN to seizure forecasting.

INDEX TERMS Epilepsy, seizure forecasting, biomedical signal processing, iEEG, sEEG, adversarial networks, neural network.

I. INTRODUCTION

Epilepsy affects almost 1% of the global population and considerably impacts the quality of life of those patients

The associate editor coordinating the review of this manuscript and approving it for publication was Venkata Rajesh Pamula^{1,2}.

diagnosed with the disease [1]–[3]. Over the past two decades, a tremendous number of techniques on predicting seizure has been proposed with promising performance. An early approach based on similarity, correlation, and energy of EEG signals achieved a modest sensitivity of 42% and a false prediction rate (FPR) less than 0.15/h tested

with the Freiburg Hospital dataset [4]. The performance improved with the use phase coherence and synchronization information in EEG signals, resulting in sensitivity 60% and FPR of 0.15/h in [5] and 95.4% and FPR of 0.36/h in [6]. A similar approach with additional features by combining bi-variate empirical mode decomposition and Hilbert-based mean phase coherence improved sensitivity to over 70% and FPR to below 0.15/h [7]. Different from the methods above, the authors in [8] used Bayesian inversion of power spectral density and then applied a rule-based decision. Their method achieved a sensitivity of 87.07% and FPR of 0.2/h on the Freiburg Hospital dataset.

Advances in machine learning have enabled major improvements in computer vision, language processing and medical applications [3]. Support vector machine (SVM) with frequency bands of the spectral energy as inputs further boosted the performance to 98.3% and FPR of 0.29/h [9] and 98% and FPR less than 0.05/h [10] test with the Freiburg Hospital dataset. In another work, features of EEG signals were estimated on a Poincaré plane using 64 fuzzy rules [11]. The features were applied principal component analysis (PCA) to reduce dimension before being classified by an SVM. This approach achieve high sensitivity of more than 91% and FPR below 0.08/h on the Freiburg Hospital dataset. In our recent work [12], we showed that convolutional neural networks (CNNs) can be used as an effective seizure prediction method.

Note that all high performance seizure forecasting algorithms were fully supervised; i.e., only labeled data were used for training. However, labeling seizure data is performed manually by neurologists and is expensive and time consuming task. There has been an increasing need to make use of unlabelled data with unsupervised feature learning such as clustering, Gaussian mixture models, Hidden Markov Models and autoencoders [13], [14]. Most of these unsupervised learning techniques have been applied to seizure detection and achieved high sensitivity and specificity [13], [15], [16]. However, there are few works successfully applying unsupervised learning in the seizure forecasting context. The authors in [17] trained unsupervised stacked autoencoders (SAE) then optimized the SAE's features with principal component analysis, independent component analysis, and differential search algorithm. These features were combined with engineered features from a priori knowledge before being classified by an SVM. This approach achieved a sensitivity of 95% and FPR of 0.06/h tested with a dataset of two epilepsy patients developed and released by the University of Pennsylvania and the Mayo Clinic. In another work, a deep convolutional autoencoder was used as unsupervised feature extractor [18]. The extracted features were fed to a bidirectional long-short term memory (Bi-LSTM) to perform the seizure prediction task. This method was tested with the CHB-MIT dataset with a sensitivity of 94.6% and a FPR of 0.04/h.

In this work, we exploit a deep convolutional generative adversarial network (GAN) [19] as an unsupervised technique to extract features from unlabeled EEG signals that can

be used for seizure forecasting task. The extracted features can be classified by any classifier (a neural network with two fully-connected layers in this work). Structure of this article is as follows. We first introduce the datasets being used in this work. Next, we describe how EEG signals are pre-processed. Then we provide details on GAN and how it can be used as a feature extractor for seizure forecasting. Lastly, we evaluate our approach and discuss the results on three datasets. A preliminary version of this work has been reported in [20]. The contribution of this paper includes:

- Confirming unsupervised feature learning using GAN for seizure forecasting is generalizable across multiple epilepsy EEG datasets,
- Bridging the gap between supervised and semi-supervised approaches,
- Linking patient-specific characteristics to seizure forecasting performance.

II. PROPOSED METHOD

A. DATASET

Table 1 summarizes the three datasets being used in this work: the CHB-MIT dataset [21], the Freiburg Hospital dataset [22], and the EPILEPSIAE dataset [23]. The CHB-MIT dataset contains scalp EEG (sEEG) data of 23 pediatric patients with 844 hours of continuous sEEG recording and 163 seizures. Scalp EEG signals were captured using 22 electrodes at a sampling rate of 256 Hz [21]. We define interictal periods that are at least 4 h away before seizure onset and after the seizure ends. In this dataset, there are cases that multiple seizures occur close to each other. For the seizure forecasting task, we are interested in predicting the leading seizures. Therefore, for seizures that are less than 30 min away from the previous one, we consider them as only one seizure and use the onset of leading seizure as the onset of the combined seizure. Besides, we only consider patients with less than 10 seizures a day for the prediction task because it is not very critical to perform the task for patients having a seizure every 2 hours on average. With the above definition and consideration, there are 13 patients with sufficient data (at least 3 leading seizures and 3 interictal hours).

TABLE 1. Summary of the three datasets used in this paper.

Dataset	EEG type	No. of patients	No. of channels	No. of seizures*	Interictal hours
Freiburg	intracranial	13	6	59	311.4
CHB-MIT	scalp	13	22	64	209
EPILEPSIAE	scalp	30	19	261	2881.4

* We are considering leading seizures only. Seizures that are less than 30 min away from the previous one are considered as one seizure only, and the onset of leading seizure is used as the onset of the combined seizure.

The Freiburg Hospital dataset consists of intracranial EEG (iEEG) recordings of 21 patients with intractable epilepsy. Due to the lack of availability of the dataset, we are only able to use data from 13 patients. A sampling rate of

256 Hz was used to record iEEG signals. In this dataset, there are 6 recording channels from 6 selected contacts where three of them are from epileptogenic regions, and the other three are from the remote regions. For each patient, there are at least 50 min preictal data and 24 h of interictal. More details about Freiburg dataset can be found in [4].

EPILEPSIAE is the largest epilepsy database that contains EEG data from 275 patients [23]. In this paper, we analyze scalp EEG of 30 patients with 261 leading seizures and 2881.4 interictal hours in total. The time-series EEG signals were recorded at a sampling rate of 256 Hz and from 19 electrodes. Seizure onset information obtained by two methods, namely EEG based and video analysis, is provided. In our study, we use seizure onset information using EEG based technique where the onsets were determined by visual inspection of EEG signals performed by an experienced clinician [23].

B. PRE-PROCESSING

Since we will use a Generative Neural Network (GAN) architecture with three de-convolution layers, dimensions of GAN's input must be divisible by 2^3 , except the number of channels. Specific to CHB-MIT dataset, some patients have less than 22 channels of recording EEG due to changes in electrodes. Particularly, Pat13 and Pat17 have only 17 available channels; Pat4, Pat9 have 20, 21 channels, respectively. Since we are interested in whether GAN can be effectively trained with non-patient specific data, all patients must have the same number of channels so that data from all patients can be combined. We follow the approach in [24] to select 16 channels for each patient in CHB-MIT dataset. With regards to CHB-MIT and Freiburg datasets, we use Short-Time Fourier Transform (STFT) to translate 28 seconds of time-series EEG signal into a two-dimensional matrix comprised of frequency and time axes. For the STFT, we use cosine window of 1-second length and 50% overlap. Most of EEG recordings were contaminated by power line noise at 60 Hz (see Fig. 1a) for CHB-MIT dataset and 50 Hz for Freiburg dataset. The power line noise can be removed by excluding components at the frequency range of 47–53 Hz and 97–103 Hz if the power frequency is 50 Hz and components at the frequency range of 57–63 Hz and 117–123 Hz for the power line frequency of 60 Hz. The DC component (at 0 Hz) was also removed. Fig. 1b shows the STFT of a 28-s window after removing power line noise. We also trim components at the last two frequencies 127–128 Hz to have the final dimension of each pre-processed 28 s be $(\text{number-of-channels} \times X \times Y) = (n \times 56 \times 112)$, where X and Y are time and frequency dimensions, respectively. n is 16, 6, 19 for the CHB-MIT dataset, the Freiburg Hospital dataset and the EPILEPSIA dataset, respectively.

C. ADVERSARIAL NEURAL NETWORK

In this paper, we use a Deep Convolutional Generative Adversarial Network (DCGAN) [19] as depicted in Fig. 2 as an unsupervised feature extraction technique. Note that here

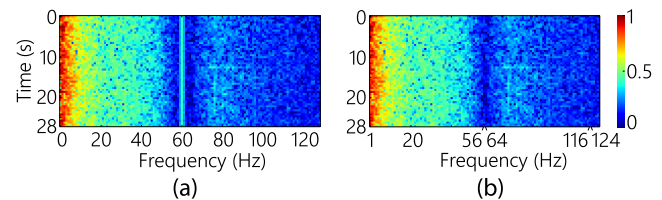


FIGURE 1. (a) Example short-time Fourier transform (STFT) of a 28-second window. (b) STFT of the same window after removing power line noise.

we explain for the CHB-MIT dataset. The same explanation is applied to the other two datasets with the change in input dimension as mentioned in Section II-B. The Generator takes a 100 dimensional sample from a uniform distribution $\mathcal{U}(-1, 1)$ as input. The input is fully-connected with a hidden layer with the output size of 6272 which is then reshaped to $64 \times 7 \times 14$. The hidden layer is followed by three de-convolution layers with filter size 5×5 , stride 2×2 . Number of filters of the three de-convolution layers are 32, 16 and n , respectively. Outputs of the Generator have the same dimension with STFT of 28 seconds EEG signals. The Discriminator, on the other hand, is configured to discriminate the generated EEG signals from the original ones. The Discriminator consists of three convolution layers with filter size 5×5 , stride 2×2 . Number of filters of the three convolution layers are 16, 32 and 64, respectively. During training, the Generator generates signals that are apparently similar to the original ones while the Discriminator is optimized to detect those generated signals. As a result, the Discriminator learns how to extract unique features in the original EEG signals by adjusting its parameters in the three convolution layers. This training process is unsupervised because we do not provide labels (preictal or interictal) to the network.

The idea of training a generative adversarial network is that the Discriminator (D) and Generator (G) compete with each other until they finally reach an equilibrium [25]. However, when we first started training the DCGAN, we observed that the Discriminator converged too fast. This prevents the Generator from learning how to generate high quality STFT samples that are not distinguishable from real STFT samples. As a result, the classification between generated STFT samples and original ones becomes a trivial task. To overcome this, we update the Generator twice instead of once every mini-batch as suggested in [26] and configure an early-stopping monitor to keep tracks of loss values of the Discriminator and Generator (defined in Eqs. 1 and 2 [25]). The monitor stops the DCGAN training if D_{loss} keeps being larger than G_{loss} over k consecutive training batches. In this work, we used $k = 20$, batch size of 64, and Adam optimizer for gradient-based learning with a learning rate of $1e^{-4}$, $\beta_1 = 0.5$, $\beta_2 = 0.999$, and $\epsilon = 1e^{-8}$. The effect of updating the Generator twice can be verified by visualizing the loss values. In Fig. 4, we plot the Discriminator and the Generator's loss values in two scenarios: update the Generator (1) once, and (2) twice every mini-batch using data of

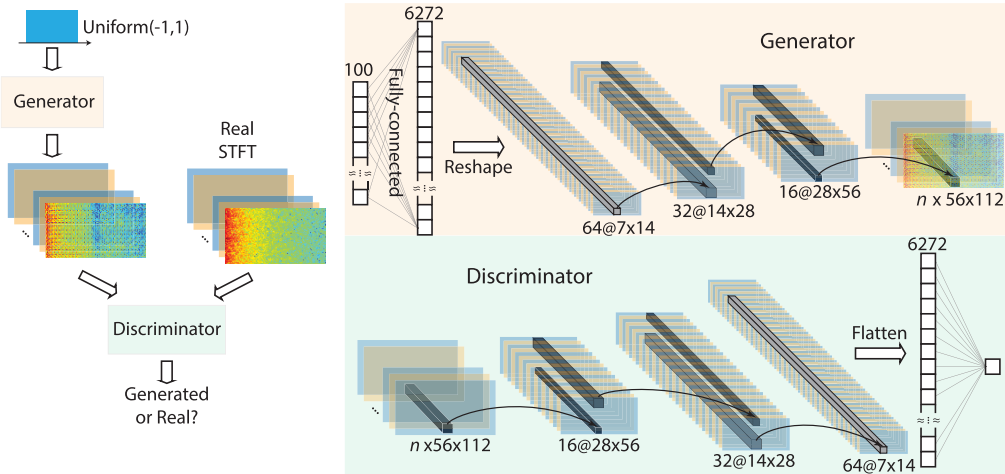


FIGURE 2. The Generator takes a random sample of 100 data points from a uniform distribution $\mathcal{U}(-1, 1)$ as input. The input is fully-connected with a hidden layer with the output size of 6272 which is then reshaped to $64 \times 7 \times 14$. The hidden layer is followed by three de-convolution layers with filter size 5×5 , stride 2×2 . Numbers of filters of the three de-convolution layers are 32, 16 and n , respectively. The Discriminator consists of three convolution layers with filter size 5×5 , stride 2×2 . Numbers of filters of the three convolution layers are 16, 32 and 64, respectively.



FIGURE 3. Seizure forecasting with features extracted by DCGAN's Discriminator. Inputs are short-time Fourier transform (STFT) of 28-s windows of raw electroencephalogram (EEG) signals. Features extracted by the three convolution blocks of the Discriminator are flattened and connected to a neural network consisting of 2 fully-connected layers with the output sizes 256 and 2, respectively. The former fully-connected layer uses sigmoid activation function while the latter uses soft-max activation function. Both of the two layers have drop-out rate of 0.5. Note that the two-layer neural network can be replaced with any other binary classifier.

Patient 1 from the CHB-MIT dataset. One can observe that the Generator's loss (G_{loss}) is lower and has less variation in scenario (2) which means the generated STFT samples better resemble the original ones. A better Generator in turn helps to improve the discriminant performance of the Discriminator. The Generator and the Discriminator reach their equilibrium after around 2000 steps where the early-stopping monitor stops the training. Note that the early-stopping was turned off when collecting loss values to produce Fig. 4.

The Discriminator's loss, D_{loss} , and the Generator's loss, G_{loss} , are defined as [25]:

$$D_{\text{loss}} = \frac{1}{m} \sum_{i=1}^m \left[\log D(x^{(i)}) + \log (1 - D(G(z^{(i)}))) \right], \quad (1)$$

$$G_{\text{loss}} = \frac{1}{m} \sum_{i=1}^m \log (1 - D(G(z^{(i)}))), \quad (2)$$

where m is the batch size (64), x is the original STFT of EEG signals, z is sampled from the distribution $\mathcal{U}(-1, 1)$.

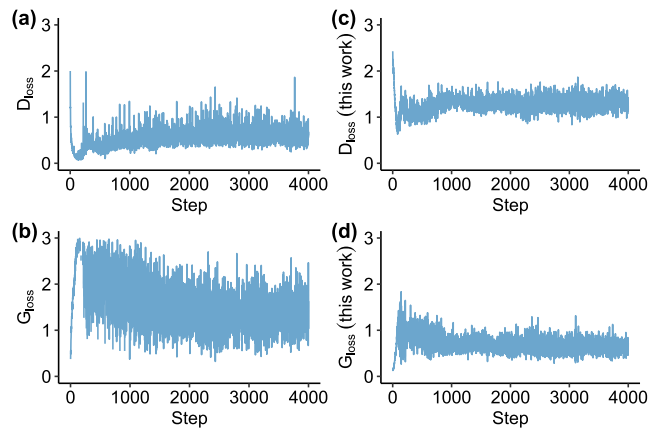


FIGURE 4. The Discriminator's and the Generator's loss values in two scenarios: update the Generator (1) once (a-b) and (2) twice (c-d) every mini-batch using data of Patient 1 from the CHB-MIT dataset.

We investigate the system performance in three scenarios: (1) GAN is trained with data of all patients combined (from the same dataset), (2) GAN is trained in a patient-specific

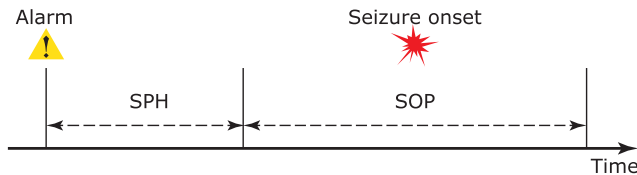


FIGURE 5. Definition of seizure occurrence period (SOP) and seizure prediction horizon (SPH). For a correct prediction, a seizure onset must be after the SPH and within the SOP.

fashion, and (3) GAN is trained in a patient-specific fashion with improvement. In scenario (3), similar to the dataset balancing technique proposed in [12], we generate extra samples from existing ones. As a result, the training set in scenario (3) is ten times larger compared to the one in scenario (2). Our model training is performed on an NVIDIA P100 graphic card using Tensorflow 1.4.0 framework.

D. SEIZURE FORECASTING WITH FEATURES

EXTRACTED BY DCGAN

We use the trained convolution layers in the DCGAN's Discriminator as a feature extractor. Specifically, we feed STFT of 28-second EEG signals into the Discriminator and collect the flatten features at its last convolution layer's output ($64 \times 7 \times 14$). Those features can now be used with any classifier to perform the seizure forecasting task. In this paper, we use a simple neural network consisting of two fully-connected layers with sigmoid activation and output sizes of 256 and 2, respectively. The former layer uses sigmoid activation function while the latter uses soft-max activation function. Both of the two layers have a drop-out rate of 0.5. The training of this two-layer neural network is patient-specific. We also apply a practice proposed in [12] to prevent over-fitting during the training of the neural network. In particular, we perform dataset balancing and then choose 25% later preictal and interictal samples from the training set to monitor if over-fitting occurs and use the rest to train the network.

E. SYSTEM EVALUATION

Seizure prediction horizon (SPH) and seizure occurrence period (SOP) need to be defined before estimating the system's performance. In this paper, we follow the definition of SOP and SPH that was proposed in [4] (see Fig. 5). SOP is the interval where the seizure is expected to occur. The period between the alarm and the beginning of SOP is called SPH. For a correct prediction, a seizure onset must be after the SPH and within the SOP. Likewise, a false alarm rises when the prediction system returns a positive but there is no seizure occurring during SOP. When an alarm rises, it will last until the end of the SOP. Regarding clinical use, SPH must be long enough to allow sufficient intervention or precautions. In contrast, SOP should be not too long to reduce the patient's anxiety.

We use area under the receiver operating characteristics curve (AUC) with SPH of 5 min and SOP of 30 min. To have a robust evaluation, we follow a leave-one-out cross-validation

approach for each subject. If a subject has N seizures, $(N - 1)$ seizures will be used for the supervised training and the withheld seizure for validation. This round is repeated N times so all seizures will be used for validation exactly one time. Interictal segments are randomly split into N parts. $(N - 1)$ parts are used for training and the rest for validation. The $(N - 1)$ parts are further split into monitoring and training sets to prevent over-fitting [12].

We compare our semi-supervised learning models with a fully-supervised approach using CNN reported in our previous work [12]. We also compare the forecasting performance with a random predictor. Specifically, we use the single-tailed Hanley-McNeil AUC test [27] to compare our AUC scores with the chance level (AUC = 0.5). The AUC values used for the Hanley-McNeil AUC test are calculated from all seizure forecasting scores during the leave-one-out cross-validation for each patient.

III. RESULTS

In this section, we test our approach with three datasets: the CHB-MIT sEEG dataset, the Freiburg Hospital iEEG dataset, and the EPILEPSIAE sEEG dataset. SOP = 30 min and SPH = 5 min were used in calculating all metrics in this paper. Each fold of leave-one-out cross-validation was executed twice, and average results with standard deviations were reported. Fig. 6 summarizes seizure forecasting results with SOP of 30 min and SPH of 5 min. Results in details are provided in Tables 2-4.

Compared to the fully supervised CNN, GAN-NN introduces $\sim 6\%$, $\sim 12\%$ and $\sim 6.6\%$ loss in AUC for the CHB-MIT sEEG dataset, the Freiburg Hospital iEEG dataset, and the EPILEPSIAE sEEG dataset, respectively. When GAN is trained per patient (GAN-PS-NN), the average AUC drops further to 72.63%, 60.91% and 63.6% for the three datasets. This can be explained by the limited amount of data from each patient. By applying $10\times$ up-sampling (GAN-PS-USPL-NN), the average AUC is boosted to 75.66% and 74.33% for the CHB-MIT dataset and the Freiburg Hospital dataset, respectively, which are 1–2% lower than those of GAN-NN. Regarding the EPILEPSIAE dataset, up-sampling technique improves overall AUC by 2% higher compared to patient-specific GAN without up-sampling (GAN-PS-NN) and 0.7% higher compared to non-patient-specific GAN (GAN-CNN). Fig. 7 demonstrates the overall seizure performance across different models and datasets. Tables 2-4 show that our seizure forecasting method is significantly better than the chance level for most of the patients at a significance level of 0.05. The supervised and semi-supervised learning methods (namely CNN, and GAN-PS-USPL-NN) outperform the random predictor for most of the patients. The percentages of patients with forecasting performance above the chance level for the two methods are (92.30%, 84.61%), (100%, 84.61%), and (86.67%, 86.67%) for the CHB-MIT dataset, the Freiburg Hospital dataset, and the EPILEPSIAE dataset, respectively.

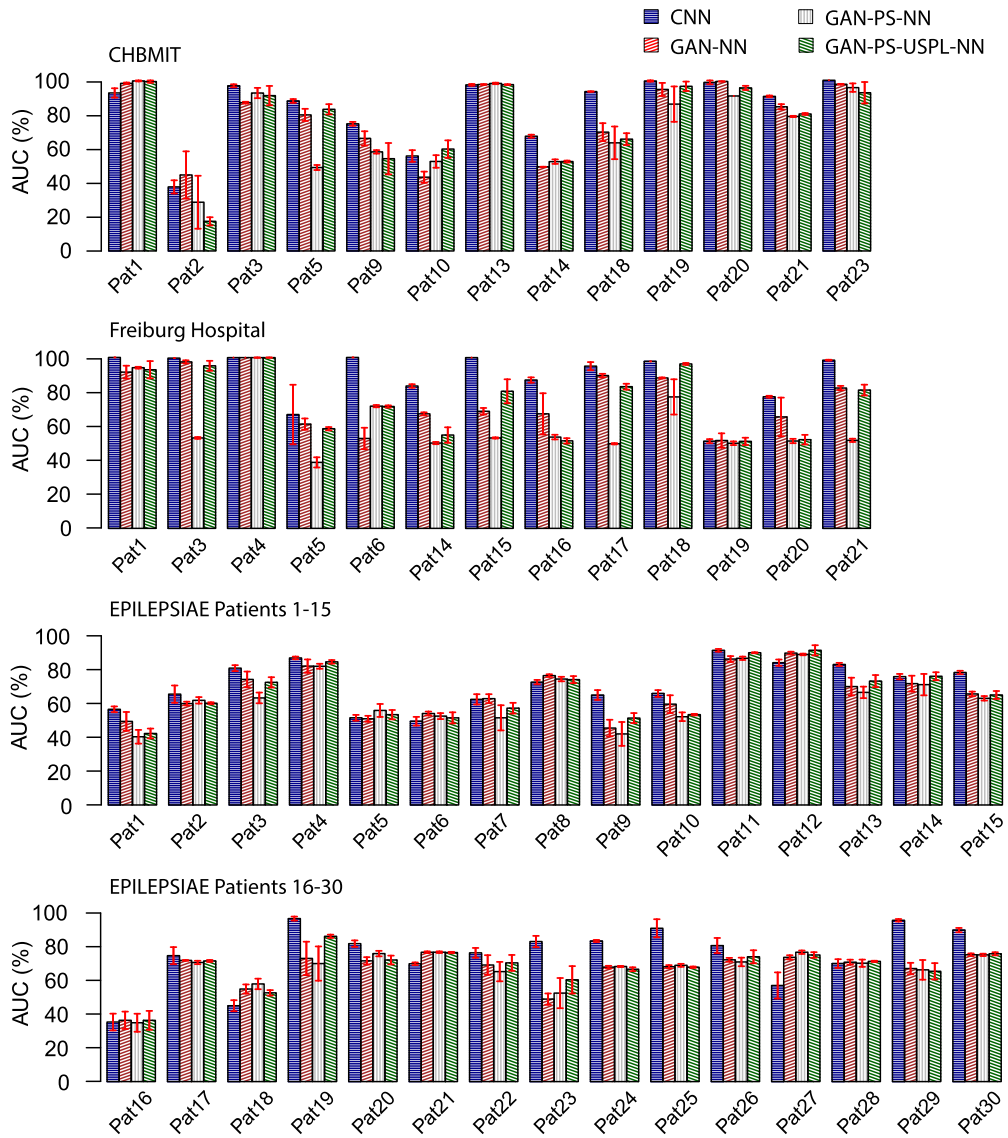


FIGURE 6. Seizure forecasting performance for the CHB-MIT dataset (upper) and the Freiburg Hospital dataset (lower). Four methods are evaluated: (1) CNN: convolutional neural network [12], (2) GAN-NN: unsupervised feature extraction using generative adversarial network (GAN) and classification performed by a two-layer neural network, (3) GAN-PS-NN similar to (2) but GAN is done patient-specific, (4) GAN-PS-USPL-NN: similar to (3) but 10× over-sampling of samples is performed when training GAN.

IV. DISCUSSION

We have shown that feature extraction for seizure forecasting can be performed in an unsupervised way. Though the overall AUC degraded by $\sim 6\text{--}12\%$ across the three datasets, our unsupervised feature extraction can help to minimize the EEG labeling task that is costly and time-consuming. Specifically, unlabeled EEG signals are used to train the GAN. The trained GAN plays like a feature extractor. Extracted features from labeled EEG data (that can be much smaller than unlabeled one) can be fed to any classifier (two fully-connected layers in our work) for the seizure forecasting task.

There is still a gap in seizure forecasting performance between fully-supervised (CNN) and semi-supervised approaches. We argue that this is because the size of training

data for GAN is not big enough. This argument is supported by the results of over-sampling data for training GAN. We have shown that over-sampling the inputs during training GAN helps to fill the gap for some patients and boost the seizure forecasting performance in overall. It is reasonable to argue that with more EEG data, the prediction accuracy can be improved. The advantage of using unsupervised feature extraction is that we can train the feature extractor (GAN) while recording EEG data, i.e., online training, without inducing extra efforts from clinicians.

Previous works using autoencoder-based unsupervised feature extraction [17], [18] achieved sensitivity higher than 94% and FPR lower than 0.06/h, which, however, cannot be directly compared with the performance of our method.

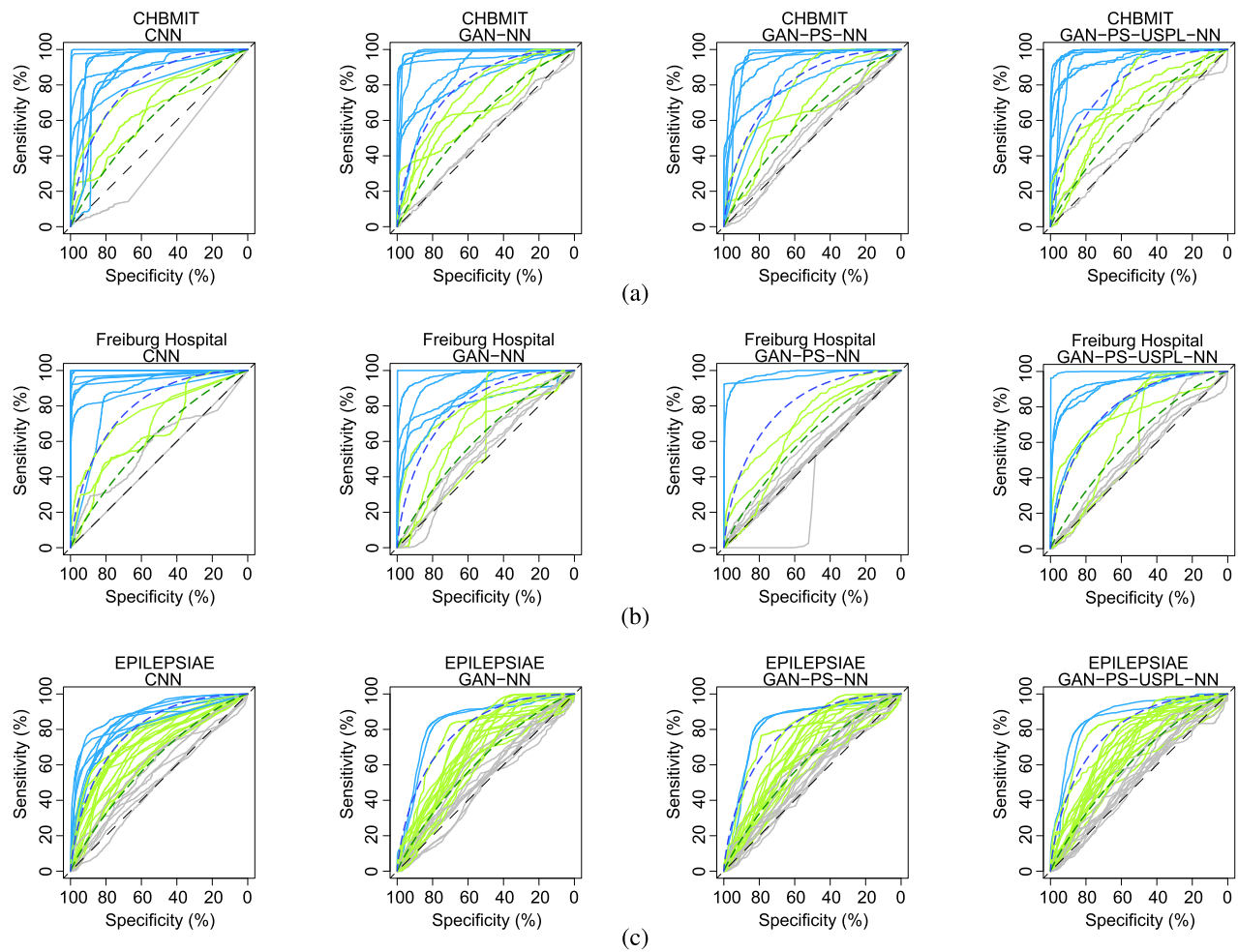


FIGURE 7. Receiver operating characteristics (ROC) curves of seizure forecasting performance testing for different patients of the three datasets: (a) - the CHB-MIT sEEG dataset, (b) - the Freiburg Hospital iEEG dataset, and (c) - the EPILEPSIAE sEEG dataset. Each line corresponds to one patient. Above the green dash line: good performance; above the blue dash line: very good performance (adapted from [1]).

TABLE 2. Seizure forecasting performance for the CHB-MIT dataset. p -values are from the single-tailed Hanley-McNeil AUC test to compare our seizure forecasting performance with the chance level ($AUC = 0.5$). Patients with p -values not being highlighted in gray color have seizure forecasting performance significantly better than the chance level with the significance level of 0.05.

Patient	CNN	p -value	GAN-NN	p -value	GAN-PS-NN	p -value	GAN-PS-USPL-NN	p -value
Pat1	92.48 ± 2.73	< 0.001	98.09 ± 0.48	< 0.001	99.52 ± 0.29	< 0.001	99.13 ± 0.68	< 0.001
Pat2	37.50 ± 3.85	1	44.47 ± 13.8	< 0.001	28.52 ± 15.4	1	17.34 ± 2.39	1
Pat3	96.66 ± 0.88	< 0.001	86.79 ± 0.51	< 0.001	92.43 ± 3.01	< 0.001	90.91 ± 5.66	< 0.001
Pat5	87.80 ± 1.09	< 0.001	79.62 ± 3.56	< 0.001	48.83 ± 1.47	0.400	82.90 ± 2.99	< 0.001
Pat9	74.41 ± 1.12	< 0.001	65.87 ± 4.18	< 0.001	57.99 ± 1.01	< 0.001	54.00 ± 9.17	< 0.001
Pat10	55.59 ± 3.39	< 0.001	43.17 ± 3.26	0.088	52.38 ± 3.67	0.028	59.63 ± 5.09	< 0.001
Pat13	97.21 ± 0.50	< 0.001	97.42 ± 0.23	< 0.001	98.04 ± 0.44	< 0.001	97.35 ± 0.25	< 0.001
Pat14	67.16 ± 0.88	< 0.001	49.22 ± 0.08	0.566	52.28 ± 1.31	0.302	52.34 ± 0.55	0.395
Pat18	93.29 ± 0.13	< 0.001	69.54 ± 5.24	< 0.001	63.27 ± 9.56	< 0.001	65.44 ± 3.47	< 0.001
Pat19	99.48 ± 0.37	< 0.001	94.53 ± 3.82	< 0.001	85.93 ± 10.3	< 0.001	96.36 ± 2.75	< 0.001
Pat20	98.67 ± 1.12	< 0.001	99.21 ± 0.08	< 0.001	90.70 ± 0.01	< 0.001	95.43 ± 1.22	< 0.001
Pat21	90.47 ± 0.50	< 0.001	84.38 ± 1.53	< 0.001	78.71 ± 0.36	< 0.001	80.17 ± 0.53	< 0.001
Pat23	99.90 ± 0.02	< 0.001	97.55 ± 0.23	< 0.001	95.59 ± 2.46	< 0.001	92.60 ± 6.26	< 0.001
Average	83.89 ± 1.28		77.68 ± 2.85		72.63 ± 3.80		75.66 ± 3.15	

The work in [17] not only utilized the unsupervised feature extraction by stacked autoencoders but also engineered features from a priori knowledge. Therefore, it is not clear how

much the extracted features from the stacked autoencoders contribute to the final performance. Also, the method was tested with only two patients with intracranial EEG signals.

TABLE 3. Seizure forecasting performance for the Freiburg Hospital dataset. *p*-values are from the single-tailed Hanley-McNeil AUC test to compare our seizure forecasting performance with the chance level (AUC = 0.5). Patients with *p*-values not being highlighted in gray color have seizure forecasting performance significantly better than the chance level with the significance level of 0.05.

Patient	CNN	<i>p</i> -value	GAN-NN	<i>p</i> -value	GAN-PS-NN	<i>p</i> -value	GAN-PS-USPL-NN	<i>p</i> -value
Pat1	100 ± 0.00	< 0.001	91.43 ± 3.75	< 0.001	94.02 ± 0.51	< 0.001	92.78 ± 5.05	< 0.001
Pat3	99.59 ± 0.00	< 0.001	97.44 ± 0.90	< 0.001	52.89 ± 0.53	0.306	95.13 ± 2.91	< 0.001
Pat4	99.93 ± 0.01	< 0.001	99.92 ± 0.01	< 0.001	99.88 ± 0.05	< 0.001	99.88 ± 0.04	< 0.001
Pat5	66.58 ± 17.4	< 0.001	61.04 ± 3.28	1	38.60 ± 2.97	1	58.28 ± 0.95	< 0.001
Pat6	100 ± 0.00	< 0.001	52.58 ± 6.26	< 0.001	71.51 ± 0.66	< 0.001	71.27 ± 0.64	< 0.001
Pat14	83.28 ± 1.02	< 0.001	67.01 ± 0.87	0.015	49.86 ± 0.65	0.044	54.60 ± 4.51	< 0.001
Pat15	99.95 ± 0.02	< 0.001	68.50 ± 1.93	< 0.001	52.88 ± 0.35	0.052	80.18 ± 7.01	< 0.001
Pat16	86.81 ± 1.53	< 0.001	67.01 ± 12.0	< 0.001	53.44 ± 1.36	1	51.17 ± 1.55	< 0.001
Pat17	94.92 ± 2.36	< 0.001	89.44 ± 1.01	< 0.001	49.49 ± 0.37	< 0.001	82.91 ± 1.70	< 0.001
Pat18	97.69 ± 0.00	< 0.001	87.99 ± 0.30	< 0.001	76.90 ± 10.3	< 0.001	96.25 ± 0.55	< 0.001
Pat19	50.97 ± 1.19	< 0.001	51.35 ± 4.19	0.991	49.77 ± 1.08	0.088	50.93 ± 2.12	0.345
Pat20	77.02 ± 0.55	< 0.001	65.24 ± 11.2	< 0.001	51.11 ± 1.27	0.677	51.91 ± 2.80	0.157
Pat21	98.40 ± 0.25	< 0.001	80.56 ± 1.26	< 0.001	51.51 ± 0.95	0.379	80.94 ± 3.16	< 0.001
Average	88.86 ± 1.87		75.35 ± 3.62		60.91 ± 1.62		74.33 ± 2.54	

TABLE 4. Seizure forecasting performance for the EPILEPSIAE dataset. *p*-values are from the single-tailed Hanley-McNeil AUC test to compare our seizure forecasting performance with the chance level (AUC = 0.5). Patients with *p*-values not being highlighted in gray color have seizure forecasting performance significantly better than the chance level with the significance level of 0.05.

Patient	CNN	<i>p</i> -value	GAN-NN	<i>p</i> -value	GAN-PS-NN	<i>p</i> -value	GAN-PS-USPL-NN	<i>p</i> -value
Pat1	56.66 ± 1.70	< 0.001	49.49 ± 5.57	0.228	40.40 ± 4.06	1	42.34 ± 2.91	1
Pat2	65.63 ± 5.12	< 0.001	60.05 ± 1.11	< 0.001	61.96 ± 1.91	< 0.001	60.24 ± 0.57	< 0.001
Pat3	81.03 ± 1.75	< 0.001	74.35 ± 4.65	< 0.001	63.39 ± 3.17	< 0.001	72.62 ± 3.04	< 0.001
Pat4	87.07 ± 0.80	< 0.001	82.23 ± 3.95	< 0.001	82.14 ± 1.48	< 0.001	84.76 ± 1.05	< 0.001
Pat5	51.64 ± 1.70	0.259	51.04 ± 1.75	0.279	55.98 ± 3.83	< 0.001	53.48 ± 2.76	< 0.001
Pat6	49.60 ± 2.57	0.975	54.16 ± 1.16	0.577	52.62 ± 1.77	1	51.59 ± 3.28	1
Pat7	62.56 ± 3.04	< 0.001	62.96 ± 2.64	< 0.001	51.62 ± 7.44	< 0.001	57.33 ± 3.16	< 0.001
Pat8	72.76 ± 1.29	< 0.001	76.61 ± 0.79	< 0.001	74.57 ± 1.33	< 0.001	74.24 ± 2.07	< 0.001
Pat9	65.12 ± 2.91	< 0.001	45.55 ± 4.91	1	42.07 ± 7.06	1	51.46 ± 2.96	0.014
Pat10	66.02 ± 1.99	< 0.001	59.70 ± 5.26	0.002	52.25 ± 2.57	0.687	53.50 ± 0.44	0.001
Pat11	91.58 ± 0.80	< 0.001	86.41 ± 1.73	< 0.001	86.87 ± 1.00	< 0.001	90.15 ± 0.30	< 0.001
Pat12	84.27 ± 1.87	< 0.001	89.94 ± 0.82	< 0.001	89.13 ± 0.48	< 0.001	91.61 ± 2.99	< 0.001
Pat13	83.21 ± 0.94	< 0.001	70.12 ± 5.24	< 0.001	66.67 ± 3.41	< 0.001	73.35 ± 3.58	< 0.001
Pat14	76.00 ± 1.60	< 0.001	71.86 ± 4.68	< 0.001	71.26 ± 6.33	< 0.001	76.23 ± 2.36	< 0.001
Pat15	78.47 ± 1.00	< 0.001	65.76 ± 1.38	< 0.001	63.16 ± 1.33	< 0.001	65.14 ± 2.34	< 0.001
Pat16	33.69 ± 4.73	1	34.67 ± 4.91	1	33.28 ± 5.09	1	34.64 ± 5.34	1
Pat17	71.22 ± 4.83	< 0.001	68.53 ± 0.22	< 0.001	67.37 ± 0.96	< 0.001	68.23 ± 0.55	< 0.001
Pat18	42.91 ± 3.12	1	52.35 ± 2.58	0.999	55.22 ± 2.98	0.030	50.20 ± 1.53	1
Pat19	92.19 ± 1.13	< 0.001	69.66 ± 9.44	< 0.001	66.74 ± 9.68	< 0.001	82.17 ± 0.94	< 0.001
Pat20	78.01 ± 1.83	< 0.001	68.28 ± 2.08	< 0.001	72.39 ± 1.55	< 0.001	68.76 ± 2.48	< 0.001
Pat21	66.62 ± 0.76	< 0.001	73.15 ± 0.49	< 0.001	73.17 ± 0.46	< 0.001	72.98 ± 0.39	< 0.001
Pat22	72.81 ± 2.77	< 0.001	65.93 ± 5.55	< 0.001	62.20 ± 5.49	< 0.001	67.14 ± 4.47	< 0.001
Pat23	79.20 ± 3.20	< 0.001	46.65 ± 3.18	1	50.04 ± 8.54	< 0.001	57.56 ± 7.74	< 0.001
Pat24	79.52 ± 0.59	< 0.001	64.73 ± 0.74	< 0.001	65.09 ± 0.33	< 0.001	63.55 ± 1.08	< 0.001
Pat25	86.71 ± 5.11	< 0.001	64.97 ± 0.88	< 0.001	65.76 ± 0.83	< 0.001	64.68 ± 0.39	< 0.001
Pat26	76.91 ± 4.31	< 0.001	68.87 ± 1.08	< 0.001	67.66 ± 2.42	< 0.001	70.58 ± 3.69	< 0.001
Pat27	54.36 ± 7.39	< 0.001	70.26 ± 1.19	< 0.001	73.16 ± 0.97	< 0.001	71.60 ± 1.58	< 0.001
Pat28	66.76 ± 2.45	< 0.001	67.51 ± 1.43	< 0.001	66.95 ± 2.04	< 0.001	67.99 ± 0.35	< 0.001
Pat29	91.22 ± 0.70	< 0.001	63.93 ± 3.24	< 0.001	63.19 ± 5.57	< 0.001	62.38 ± 4.61	< 0.001
Pat30	85.67 ± 1.21	< 0.001	71.72 ± 0.75	< 0.001	71.66 ± 0.66	< 0.001	72.28 ± 0.86	< 0.001
Average	71.65 ± 2.44		65.05 ± 2.78		63.60 ± 3.16		65.76 ± 2.33	

The other work in [18] defined preictal period right next to ictal period which means seizure prediction period (SPH) is zero. However, from a clinical perspective, SPH needs to be long enough to allow sufficient intervention [12].

In the field of computer vision, GAN can help to reduce the amount of labeled data without compromising the classification performance [28]. Unfortunately, with the current sizes of the datasets available to us, we could not replicate a similar

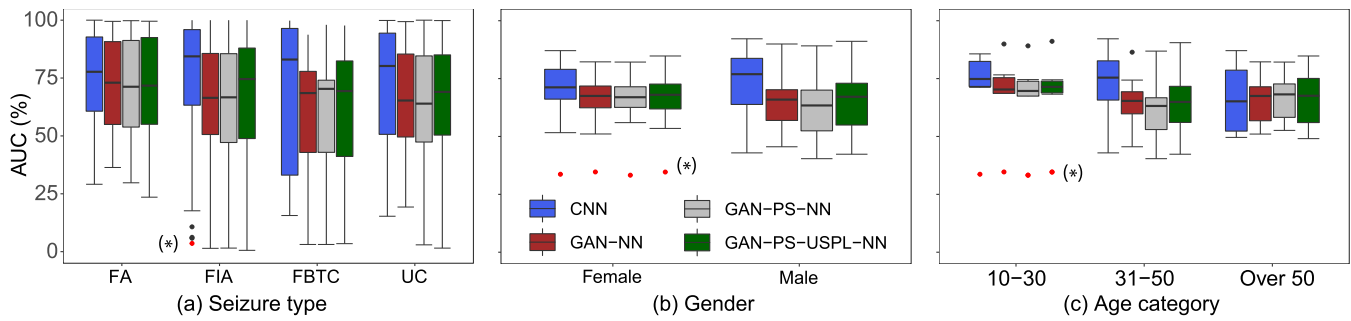


FIGURE 8. Seizure forecasting performance (AUC) across different patient-specific characteristics for the EPILEPSIAE dataset: (a) - Seizure type, (b) - Gender, (c) - Age. Refer to Table 5 for the patients' details. Dots indicate outliers. Data points in red (*) are from the same patient. FA: focal aware, FIA: focal impaired awareness, FBTC: focal to bilateral tonic-clonic, UC: unclassified.

TABLE 5. The EPILEPSIAE scalp EEG dataset.

Patient	Gender	Age	No. of seizures	No. of leading seizures*	Interictal hours
Pat1	male	36	11	11	68.9
Pat2	female	46	8	8	114.9
Pat3	male	41	8	8	96.3
Pat4	female	67	5	5	126
Pat5	female	52	8	8	204.1
Pat6	male	65	8	7	92.2
Pat7	male	36	5	5	75.7
Pat8	male	26	22	11	65.6
Pat9	male	47	6	6	51.1
Pat10	male	44	11	11	60.7
Pat11	male	48	14	14	57.8
Pat12	male	28	9	9	94.1
Pat13	male	46	8	8	101.3
Pat14	female	62	6	6	115.7
Pat15	female	41	5	5	82.8
Pat16	female	15	6	6	51.1
Pat17	female	17	9	9	82.4
Pat18	male	47	7	6	133
Pat19	male	32	22	21	75.4
Pat20	male	47	7	7	115.3
Pat21	female	31	8	8	106.6
Pat22	male	38	7	7	88.2
Pat23	male	50	9	9	179.6
Pat24	female	54	10	10	36.2
Pat25	male	42	8	8	109.8
Pat26	male	13	9	9	97.1
Pat27	male	58	9	8	99.9
Pat28	female	35	9	9	95.2
Pat29	male	50	10	10	111.9
Pat30	female	16	12	12	92.5

* We are considering leading seizures only. Seizures that are less than 30 min away from the previous one are considered as one seizure only and the onset of leading seizure is used as the onset of the combined seizure.

claim for seizure forecasting using GAN as an unsupervised feature extractor.

Another aspect that we believe it is important is that how patient-specific characteristics, such as seizure types [2], [29], age, and gender, affects seizure forecasting performance testing with the EPILEPSIAE dataset. In this dataset, seizures are categorized into focal aware (simple partial), focal impaired awareness (complex partial), focal to bilateral tonic-clonic (secondarily generalized tonic-clonic)

and unclassified. Age of the patients is ranging from 13 to 67. In terms of seizure type, focal aware seizures have the least variation in seizure forecasting. This observation could be helpful for clinical trial consideration; e.g., focus on patients with focal aware seizures first. Regarding the gender, seizure forecasting is better for female patients overall, with an exception that there is one female who has a very low AUC score (below 35%). It is most interesting to observe that patients with age in the range of 10 to 30 have considerably higher AUC score and less variation compared to other groups. In fact, if we exclude the patient with very low AUC score which is an outlier from group 10 to 30, it can be seen that seizures of young patients (30 and below) can be predicted with the highest accuracy. The reason behind this observation is not clear and is not in the scope of this article.

V. CONCLUSION

Seizure forecasting capability has been studied and improved over the last four decades. A perfect prediction is yet available but with current prediction performance, it is useful to provide the patients with warning message so they can take some precautions for their safety. We have shown that feature extraction for seizure forecasting can be done using unsupervised deep learning or GAN particularly. Using semi-supervised seizure forecasting approach, 61.53% of the patients in the CHB-MIT dataset, 53.84% in the Freiburg Hospital dataset and 13.33% in the EPILEPSIAE dataset have very good seizure forecasting performance (with AUC above 80%). Through our observations regarding patient-specific characteristics, it is suggested that female patients under thirty years old with focal aware seizure type would benefit the most from such a seizure forecasting system.

REFERENCES

- [1] L. Kuhlmann, K. Lehnertz, M. P. Richardson, B. Schelter, and H. P. Zaveri, "Seizure prediction—Ready for a new era," *Nature Rev. Neurol.*, vol. 14, no. 10, pp. 618–630, Aug. 2018.
- [2] R. S. Fisher, J. H. Cross, J. A. French, N. Higurashi, E. Hirsch, F. E. Jansen, L. Lagae, S. L. Moshé, J. Peltola, E. R. Perez, I. E. Scheffer, and S. M. Zuberi, "Operational classification of seizure types by the International League Against Epilepsy: Position paper of the ILAE commission for classification and terminology," *Epilepsia*, vol. 58, no. 4, pp. 522–530, 2017.

- [3] L. Kuhlmann *et al.*, "Epilepsyecosystem.org: Crowd-sourcing reproducible seizure prediction with long-term human intracranial EEG," *Brain*, vol. 141, no. 9, pp. 2619–2630, 2018.
- [4] T. Maiwald, M. Winterhalder, R. Aschenbrenner-Scheibe, H. U. Voss, A. Schulze-Bonhage, and J. Timmer, "Comparison of three nonlinear seizure prediction methods by means of the seizure prediction characteristic," *Phys. D, Nonlinear Phenomena*, vol. 194, nos. 3–4, pp. 357–368, 2004.
- [5] M. Winterhalder, B. Schelter, T. Maiwald, A. Brandt, A. Schad, A. Schulze-Bonhage, and J. Timmer, "Spatio-temporal patient-individual assessment of synchronization changes for epileptic seizure prediction," *Clin. Neurophysiol.*, vol. 117, no. 11, pp. 2399–2413, Nov. 2006.
- [6] M. Z. Parvez and M. Paul, "Seizure prediction using undulated global and local features," *IEEE Trans. Biomed. Eng.*, vol. 64, no. 1, pp. 208–217, Jan. 2017.
- [7] Y. Zheng, G. Wang, K. Li, G. Bao, and J. Wang, "Epileptic seizure prediction using phase synchronization based on bivariate empirical mode decomposition," *Clin. Neurophysiol.*, vol. 125, no. 6, pp. 1104–1111, Jun. 2014.
- [8] A. Aarabi and B. He, "Seizure prediction in hippocampal and neocortical epilepsy using a model-based approach," *Clin. Neurophysiol.*, vol. 125, no. 5, pp. 930–940, May 2014.
- [9] Y. Park, L. Luo, K. K. Parhi, and T. Netoff, "Seizure prediction with spectral power of EEG using cost-sensitive support vector machines," *Epilepsia*, vol. 52, no. 10, pp. 1761–1770, 2011.
- [10] Z. Zhang and K. K. Parhi, "Low-complexity seizure prediction from iEEG/sEEG using spectral power and ratios of spectral power," *IEEE Trans. Biomed. Circuits Syst.*, vol. 10, no. 3, pp. 693–706, Jun. 2016.
- [11] B. Sharif and A. H. Jafari, "Prediction of epileptic seizures from EEG using analysis of ictal rules on Poincaré plane," *Comput. Methods Programs Biomed.*, vol. 145, pp. 11–22, Jul. 2017.
- [12] N. D. Truong, A. D. Nguyen, L. Kuhlmann, M. R. Bonyadi, J. Yang, S. Ippolito, and O. Kavehei, "Convolutional neural networks for seizure prediction using intracranial and scalp electroencephalogram," *Neural Netw.*, vol. 105, pp. 104–111, Sep. 2018.
- [13] O. Smart and M. Chen, "Semi-automated patient-specific scalp EEG seizure detection with unsupervised machine learning," in *Proc. IEEE Conf. Comput. Intell. Bioinform. Comput. Biol.*, Aug. 2015, pp. 1–7.
- [14] T. Wen and Z. Zhang, "Deep convolution neural network and autoencoders-based unsupervised feature learning of EEG signals," *IEEE Access*, vol. 6, pp. 25399–25410, 2018.
- [15] P. A. Bizopoulos, D. G. Tsalikakis, A. T. Tzallas, D. D. Koutsouris, and D. I. Fotiadis, "EEG epileptic seizure detection using k-means clustering and marginal spectrum based on ensemble empirical mode decomposition," in *Proc. IEEE Int. Conf. BioInform. BioEng.*, Nov. 2013, pp. 1–4.
- [16] A. Supratak, L. Li, and Y. Guo, "Feature extraction with stacked auto-encoders for epileptic seizure detection," in *Proc. Int. Conf. Eng. Med. Biol. Soc.*, Aug. 2014, pp. 4184–4187.
- [17] M.-P. Hosseini, D. Pomplini, K. Elisevich, and H. Soltanian-Zadeh, "Optimized deep learning for EEG big data and seizure prediction BCI via Internet of Things," *IEEE Trans. Big Data*, vol. 3, no. 4, pp. 392–404, Dec. 2017.
- [18] A. Abdelhameed and M. Bayoumi, "Semi-supervised deep learning system for epileptic seizures onset prediction," in *Proc. IEEE Int. Conf. Mach. Learn. Appl.*, Dec. 2018, pp. 1186–1191.
- [19] A. Radford, L. Metz, and S. Chintala, "Unsupervised representation learning with deep convolutional generative adversarial networks," 2015, *arXiv:1511.06434*. [Online]. Available: <https://arxiv.org/abs/1511.06434>
- [20] N. D. Truong, L. Zhou, and O. Kavehei, "Semi-supervised seizure prediction with generative adversarial networks," in *Proc. 41st Annu. Int. Conf. IEEE Eng. Med. Biol. Soc. (EMBC)*, Berlin, Germany, Jul. 2019.
- [21] A. H. Shoeb, "Application of machine learning to epileptic seizure onset detection and treatment," Ph.D. dissertation, Harvard Univ.-MIT Division Health Sci. Technol., Cambridge, MA, USA, 2009.
- [22] University Hospital of Freiburg. (2003). *EEG Database at the Epilepsy Center of the University Hospital of Freiburg, Germany*. [Online]. Available: <http://epilepsy.uni-freiburg.de>
- [23] J. Klatt, H. Feldwisch-Drentrup, M. Ihle, V. Navarro, M. Neufang, C. Teixeira, C. Adam, M. Valderrama, C. Alvarado-Rojas, A. Witon, M. Le Van Quyen, F. Sales, A. Dourado, J. Timmer, A. Schulze-Bonhage, and B. Schelter, "The EPILEPSIAE database: An extensive electroencephalography database of epilepsy patients," *Epilepsia*, vol. 53, no. 9, pp. 1669–1676, 2012.
- [24] N. D. Truong, L. Kuhlmann, M. R. Bonyadi, J. Yang, A. Faulks, and O. Kavehei, "Supervised learning in automatic channel selection for epileptic seizure detection," *Expert Syst. Appl.*, vol. 86, pp. 199–207, Nov. 2017.
- [25] I. Goodfellow, J. Pouget-Abadie, M. Mirza, B. Xu, D. Warde-Farley, S. Ozair, A. Courville, and Y. Bengio, "Generative adversarial nets," in *Proc. Adv. Neural Inf. Process. Syst.*, 2014, pp. 2672–2680.
- [26] S.-H. Sun. (2017). *Deep Convolutional Generative Adversarial Networks in Tensorflow*. [Online]. Available: <https://github.com/shaohua0116/DCGAN-Tensorflow>
- [27] J. A. Hanley and B. J. McNeil, "A method of comparing the areas under receiver operating characteristic curves derived from the same cases," *Radiology*, vol. 148, no. 3, pp. 839–843, 1983.
- [28] D. P. Kingma, S. Mohamed, D. J. Rezende, and M. Welling, "Semi-supervised learning with deep generative models," in *Proc. Adv. Neural Inf. Process. Syst.*, 2014, pp. 3581–3589.
- [29] A. J. Espay, S. Aybek, A. Carson, M. J. Edwards, L. H. Goldstein, M. Hallett, K. LaFaver, W. C. LaFrance, A. E. Lang, T. Nicholson, and G. Nielsen, "Current concepts in diagnosis and treatment of functional neurological disorders," *JAMA Neurol.*, vol. 75, no. 9, pp. 1132–1141, 2018.



NHAN DUY TRUONG (S'16) received the B.Eng. degree in electronics and telecommunications with Gold Medal for Top Graduate from the Ho Chi Minh City University of Technology, Vietnam, in 2010, and the M.Eng. degree in electronics and computer engineering from the Royal Melbourne Institute of Technology, in 2013. He is currently pursuing the Ph.D. degree with the Faculty of Engineering, The University of Sydney, Australia. His current research interests include neural networks, medical devices, deep learning, and its hardware implementation. He was a recipient of the John Makepeace Bennett Gift Scholarship through the Australian Institute for Nanoscale Science and Technology (AINST) and administered by the University of Sydney Nano Institute.



LEVIN KUHLMANN received the Ph.D. degree in cognitive and neural systems from Boston University, in 2007. He was a Researcher with the Centre for Human Pharmacology, Swinburne University of Technology, Melbourne, and the Departments of Electrical and Electronic Engineering, Biomedical Engineering and Medicine, The University of Melbourne. He is currently a Senior Lecturer with the Faculty of Information Technology, Monash University. He is also with the Department of Medicine, St. Vincent's Hospital Melbourne, The University of Melbourne. His current research interests include signal processing, control theory, machine learning, statistics and computational neuroscience applications to digital health, neural engineering, and neuroimaging and medicine.



MOHAMMAD REZA BONYADI (M'14–SM'18) received the Ph.D. degree in math and computer sciences from The University of Adelaide, Australia. He is currently with the Data Science and Artificial Intelligence Team, Rio Tinto, Brisbane, Australia, and also an Honorary Adjunct Researcher with the Centre for Advanced Imaging, The University of Queensland, Queensland, Australia, and the Optimization and Logistics Group, The University of Adelaide. His current research interests include theory and applications of optimization and machine learning. During his career, he has published over 50 articles in top international journals, conferences, and chapter of books in the field of optimization, pattern recognition, and machine learning. He has been involved as a committee member, organizer, or reviewer in over 50 international journals and conferences in the field of optimization and machine learning.



DAMIEN QUERLOZ (M'08) received the predoctoral education from the Ecole Normale Supérieure, Paris, and the Ph.D. degree from the Université Paris-Sud, in 2008. After postdoctoral appointments at Stanford University and CEA, he became a permanent Researcher with the Centre for Nanoscience and Nanotechnology, Université Paris-Sud. He is currently a CNRS Research Scientist with Univeristé Paris-Sud. He focuses on novel usages of emerging non-volatile memory, in particular relying on inspirations from biology and machine learning. He coordinates the INTEGNANO Interdisciplinary Research Group. In 2016, he was a recipient of the European Research Council Starting Grant to develop the concept of natively intelligent memory. He also received the CNRS Bronze Medal, in 2017.



OMID KAVEHEI (S'05–M'12–SM'16) received the Ph.D. degree in electronics from the University of Adelaide, in 2012, with the Post-graduate University Alumni Medal, a University Doctoral Research Medal, and the 2011 South Australian Young Nanotechnology Ambassador Award. He was with the Centre for Neural Engineering, The University of Melbourne, as a Research Fellow in microelectronics, where he involved in an Australian engineering flagship project, the Bionic Eye. He was a Visiting Project Scientist with the University of California Santa Barbara, Santa Barbara, CA, USA. He is currently a Senior Lecturer, a SOAR Fellow, and a Deputy Director of The University of Sydney Nano Institute. He is also with the Faculty of Engineering, The University of Sydney. His current research interests include neuromorphic computing for biomedical signal processing and emerging applications of nanoelectronics.



LUPING ZHOU (M'11–SM'13) received the B.Eng., M.Sc., and Ph.D. degrees from Southeast University, China, National University of Singapore, and Australian National University, respectively. She did the postdoctoral training with the University of North Carolina, Chapel Hill, NC, USA. She is currently a Senior Lecturer and ARC DECRA Fellow with the School of Electrical and Information Engineering, The University of Sydney, Australia. Her current research interests include medical image analysis, machine learning, and computer vision. Her current research is focused on medical image analysis with statistical graphical models and deep learning.